Physicochemical Characterization of New Octamethylferrocenylmethylenemalononitrile by Complementary Methods: UV−Visible Solvatochromism, Moessbauer Spectroscopy, Differential Scanning Calorimetry, and X-ray Structure Determination

Gerhard Laus*

Immodal Pharmaka GmbH, Bundesstrasse 44, A-6111 Volders, Austria

Herwig Schottenberger* and Klaus Wurst

Institute of Inorganic Chemistry, University of Innsbruck, Innrain 52a, A-6020 Innsbruck, Austria

Rolfe H. Herber*

The Racah Institute of Physics, The Hebrew University of Jerusalem, 91904 Jerusalem, Israel

Ulrich Griesser

Institute of Pharmacy, University of Innsbruck, Innrain 52a, A-6020 Innsbruck, Austria

Received: January 21, 2004; In Final Form: February 18, 2004

(Octamethylferrocenylmethylene)malononitrile (dicyanoethenyl-octamethylferrocene) was synthesized by condensation of octamethylferrocene carbaldehyde with malononitrile. The visible positive solvatochromism of the new compound was studied in 33 solvents and discussed in terms of Kamlet−Taft's π^* and α scales. Temperature-dependent Moessbauer spectroscopy using a ^{57}Fe-enriched sample suggests that the onset of ring rotation of the tetramethyl Cp ring was not accompanied by a significant librational motion of the ring. The quadrupole splitting parameter went through a maximum at ∼220 K suggesting a phase change in the solid. Differential scanning calorimetry showed two endotherms at 228 and 236 K. Single crystal X-ray structure determinations at different temperatures showed two kinds of disorder at 243 K, only one of which remained at 183 K. A reversible change of disorder was observed at 213 K.

Introduction

Metallocene-based donor−acceptor chromophores are widely investigated for their linear and nonlinear optical properties.[1−3] The relationships between electronic structure and optical properties of conjugated metallocene derivatives were recently surveyed.[4] Introduction of methyl substituents into the cyclopentadienide (Cp) rings increases the donor strength of the metallocene and gives rise to interesting dynamic behavior, as observed by temperature-dependent Moessbauer spectroscopy.[5] Variation of the acceptor strength also affects the spectral properties.[3] Dicyanoethenyl and bis(dicyanoethenyl) systems[6] were previously used as strong electron-accepting groups. The solvatochromism[7] of the characteristic intramolecular charge-transfer bands can be interpreted using multiparameter solvent polarity scales. In the course of our ongoing studies of dipolar compounds in solution[8] and in solid state,[9] a simple synthesis[1] of the novel (octamethylferrocenylmethylene)malononitrile (**1**) is reported, and spectroscopical and structural properties of this new compound are presented.

Experimental Section

Materials. ^{57}Fe-enriched iron powder (>95%) was purchased from Advanced Materials Technologies, Israel. All solvents were of spectroscopic grade.

Equipment and Methods. Electronic absorption spectra were recorded on a Shimadzu UV-160A spectrophotometer at 298 K. The wavelength scale was calibrated using a solution of holmium perchlorate. All measurements were taken at least in triplicate and averaged. High-resolution mass spectra were measured with a Finnigan MAT 95 spectrometer. NMR spectra were recorded on a Bruker AC 300 spectrometer using tetramethylsilane as reference. IR spectra were measured with a Bruker IFS25 FTIR spectrometer, and Raman spectra were recorded on a Bruker RFS100 spectrometer. Temperature-dependent ^{57}Fe Moessbauer spectra were acquired in transmission mode, using a ^{57}Co in Rh matrix source at room temperature. Spectrometer calibration was effected using an α-Fe absorber at room temperature, and all isomer shifts are reported with respect to the centroid of these calibration spectra. A sample of the ^{57}Fe enriched title compound was plated out onto a plastic sample holder from diethyl ether solution, thoroughly vacuum-dried, and subjected to temperature-dependent Moessbauer study as described previously.[10] Differential scanning calorimetric measurements were performed with a Mettler Toledo Star System model DSC 821 instrument in the warming mode at 5 degrees per minute. The ambient environment was nitrogen boil-off gas, and the sample size was 6.50 mg. X-ray powder diffractograms were aquired with a Siemens D5000 diffractometer (Cu Kα radiation). Diffraction intensity data of single crystals were collected by means of a Nonius Kappa CCD with graphite-monochromatized Mo Kα radiation via ϕ and ω scans.

* To whom correspondence should be addressed. E-mail: (G.L.) gerhardlaus@hotmail.com; (H.S.) herwig.schottenberger@uibk.ac.at; (R.H.H.) herber@vms.huji.ac.il.

10.1021/jp049698j CCC: $27.50
Published on Web 03/26/2004

SCHEME 1: Reaction Scheme of the Synthesis of 1

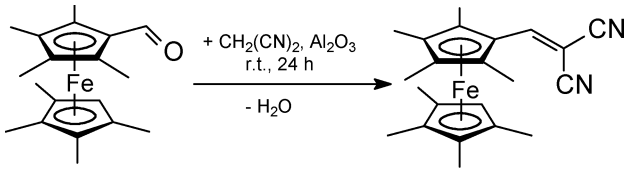

1

The structures were solved with direct methods (SHELXS-86) and refined against F^2 (SHELXL-97).

Synthesis. Enriched $^{57}FeCl_2$ was prepared from ^{57}Fe by a modified[11] literature procedure.[12] Both enriched and natural abundance octamethylferrocene carbaldehyde were prepared from $FeCl_2$ by complexation with $CpMe_4$ anion[13] and subsequent formylation.[14] Condensation with malononitrile was achieved by the very simple and efficient method of Toma and coworkers[1] using basic alumina in a solvent-free reaction (Scheme 1) which is well-suited for small scale preparations. The products were purified by repeated chromatography (basic alumina with 5% water, a. diethyl ether, b. dichloromethane).

Data for **1**. Yield: 32%. mp. 109 °C. HRMS (EI): *m*/*z* 374.1454 (calc. for $C_{22}H_{26}N_2Fe$: 374.1445). ^1H NMR ($CDCl_3$, TMS): δ 1.62 (6H, s), 1.67 (6H, s), 1.88 (6H, s), 1.96 (6H, s), 3.47 (1H, s), 7.55 (1H, s) ppm. ^{13}C NMR ($CDCl_3$, TMS): δ 9.3, 9.9, 11.1, 12.3, 72.5, 74.5, 75.1, 83.2, 88.9, 115.3, 116.5, 163.7 ppm. IR (KBr): 2960, 2910, 2220, 1565, 1335, 1030 cm^{-1}. Raman (neat): 2220, 1565 cm^{-1}.

Data for [^{57}Fe]**1**. HRMS (EI): *m*/*z* 375.1434 (calc. for $C_{22}H_{26}N_2{}^{57}Fe$: 375.1444). NMR spectra were identical with those of unlabeled **1**.

Crystal data of **1** at $T = 183$ K. Blue prism (0.25 × 0.15 × 0.11 mm) from diethyl ether, triclinic, $a = 1546.44(6)$, $b = 1552.48(4)$, $c = 1843.54(8)$ pm, $\alpha = 102.861(2)$, $\beta = 104.736(2)$, $\gamma = 104.130(2)°$, $V = 3.9551(3)$ nm^3, space group P-1 (no. 2), $Z = 8$, $\mu = 0.768$ mm^{-1}, 18302 reflections measured, 10310 independent ($R_{int} = 0.0299$), 7941 observed, $R_1 = 0.0480$ and $wR_2 = 0.1213$ ($I > 2\sigma(I)$), $R_1 = 0.0685$ and $wR_2 = 0.1319$ (all data), goodness of fit 1.061.

Crystal data of **1** at $T = 243$ K. Blue prism (0.25 × 0.15 × 0.11 mm) from diethyl ether, triclinic, $a = 1054.72(3)$, $b = 1347.17(4)$, $c = 1513.97(4)$ pm, $\alpha = 83.391(2)$, $\beta = 72.174(2)$, $\gamma = 79.825(2)°$, V=2.01142(10) nm^3, space group P-1 (no. 2), $Z = 4$, $\mu = 0.755$ mm^{-1}, 10379 reflections measured, 5932 independent (R_{int}=0.0230), 4833 observed, $R_1 = 0.0455$ and $wR_2 = 0.1133$ ($I > 2\sigma(I)$), $R_1 = 0.0598$ and $wR_2 = 0.1208$ (all data), goodness of fit 1.044.

CCDC 227351 and 227352 contain the supplementary crystallographic data for this paper. These data can be obtained free of charge via www.ccdc.cam.ac.uk/conts/retrieving.html (or from the Cambridge Crystallographic Data Centre, 12, Union Road, Cambridge CB2 1EZ, United Kingdom; fax: +44 1223 336033; or deposit@ccdc.cam.ac.uk).

Results and Discussion

Solvatochromism in Electronic Absorption Spectra. Compound **1** exhibits visible positive solvatochromism: purple in *n*-heptane and blue in dimethyl sulfoxide. The absorption spectrum shows two bands in the UV−visible region (Figure 1). The high-energy transition is assigned to an intraligand charge transfer and the low-energy transition to a metal-to-ligand charge-transfer excitation.[15] The high-energy band is shifted bathochromically by $\Delta\lambda = 12$ nm and the low-energy band by

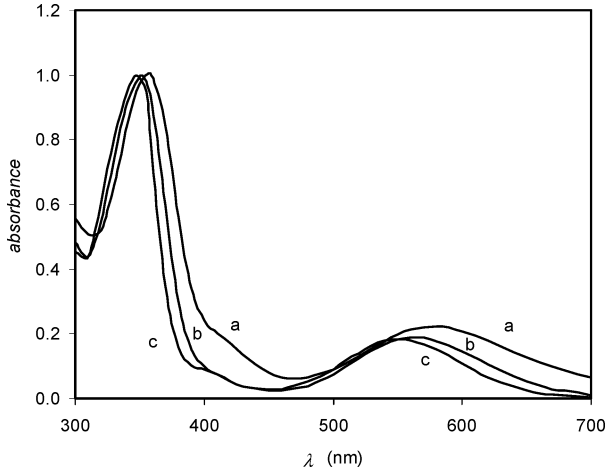

Figure 1. Normalized electronic absorption spectra of **1** in (a) dichloromethane, (b) ethyl acetate, and (c) cyclohexane.

$\Delta\lambda = 25$ nm on changing the solvent from *n*-heptane to dimethyl sulfoxide, indicative of increased polarity in the excited state. This solvatochromic shift is slightly less than the one observed for the related 2-nitro-3-(octamethylferrocenyl)acrylonitrile[9] ($\lambda_{max} = 376$ and 598 nm in *n*-heptane and 408 and 646 nm in DMSO). As expected, both transitions are blue-shifted when the nitro is replaced by a cyano group. The electronic absorption maxima in 33 solvents of different polarity and the corresponding molar transition energies E_T, as calculated by eq 1, are summarized in Table 1. Molar absorption coefficients ϵ in dichloromethane are also included.

$$E_T(\text{kJ mol}^{-1}) = hcN/\lambda = 119\,625/\lambda(\text{nm}) \quad (1)$$

A linear solvation energy relationship was established by least-squares fitting the data to the simplified solvatochromic eq 2[16] involving only the parameters π^*[17] and α[18] which represent the dipolarity/polarizability and hydrogen-bond donor (HBD) capability of the solvent.

$$E_T = E_{T0} + s\pi^* + a\alpha \quad (2)$$

The coefficients *s* and *a* reflect the sensitivity of the solute to these solvent properties. The hydrogen-bond acceptor (HBA) parameter β[19] did not significantly contribute to the relationship. From the spectral data, the following equations (3 and 4) were derived by multiple linear regression (standard errors of E_{T0}, *s*, and *a*, squared correlation coefficient r^2 of calculated vs. found values, residual standard deviation σ of the correlation, and number *N* of data points given) which adequately describe the solvatochromic behavior of compound **1**:

$$E_{T1}(\text{kJ mol}^{-1}) = (345.36 \pm 0.50) - (12.37 \pm 0.80)\pi^* - (3.24 \pm 0.57)\alpha \quad (3)$$

$$r^2 = 0.906,\ \sigma(\text{kJ mol}^{-1}) = 1.18\ (\text{rel. } \sigma = 0.35\%),\ N = 31$$

$$E_{T2}(\text{kJ mol}^{-1}) = (216.44 \pm 0.33) - (9.70 \pm 0.51)\pi^* - (3.35 \pm 0.39)\alpha \quad (4)$$

$$r^2 = 0.935,\ \sigma(\text{kJ mol}^{-1}) = 0.79\ (\text{rel. } \sigma = 0.38\%),\ N = 33$$

The *s*/*a* ratios are 3.82 and 2.90, respectively, which are significantly lower than those of the related 2-nitro-3-(octamethylferrocenyl)acrylonitrile (9.9 and 7.5), indicating that the dinitrile **1** is more sensitive to hydrogen bonding and less sensitive to the dipolarity/polarizability of the solvent than the

TABLE 1: Electronic Absorption Maxima and Molar Transition Energies for 1 in Different Solvents

solvent	π^* [a]	α[a]	λ_{max1} (nm)	E_{T1} (kJ mol^{-1})	λ_{max2} (nm)	E_{T2} (kJ mol^{-1})
formic acid	0.65	1.23	360.1	332.2	585.0	204.5
methanol	0.60	0.98	355.8	336.2	573.3	208.7
ethanol	0.54	0.86	355.6	336.4	572.8	208.9
1-propanol	0.52	0.84	355.0	337.0	571.6	209.3
1-butanol	0.47	0.84	355.4	336.6	571.3	209.4
2-propanol	0.48	0.76	355.6	336.4	571.3	209.4
2-butanol	0.40	0.69	355.0	337.0	573.3	208.6
acetonitrile	0.75	0.19	355.0	337.0	572.0	209.1
dichloromethane	0.82	0.13	358.9 [b]	333.3	575.0 [c]	208.0
acetone	0.71	0.08	354.2	337.8	570.9	209.5
2-butanone	0.67	0.06	353.9	338.1	569.1	210.2
diiodomethane	1.12	0	*d*		581.1	205.9
dimethyl sulfoxide	1.00	0	358.7	333.5	576.0	207.7
dimethylformamide	0.88	0	357.5	334.7	574.7	208.2
dimethylacetamide	0.88	0	356.3	335.7	573.2	208.7
pyridine	0.87	0	359.0	333.2	576.3	207.6
1,2-dichlorobenzene	0.80	0	358.6	333.6	575.9	207.7
propionitrile	0.71	0	354.8	337.1	572.1	209.1
chlorobenzene	0.71	0	356.6	335.4	574.1	208.4
carbon disulfide	0.61	0	*d*		567.3	210.9
benzene	0.59	0	355.6	336.4	569.6	210.0
tetrahydrofuran	0.58	0	353.3	338.6	566.1	211.3
ethyl acetate	0.55	0	352.0	339.8	564.6	211.9
toluene	0.54	0	355.0	337.0	567.5	210.8
1,2-dimethoxyethane	0.53	0	354.0	337.9	567.4	210.8
trichloroethylene	0.53	0	354.0	337.9	570.8	209.6
n-butyl acetate	0.46	0	350.5	341.3	564.5	211.9
tetrachloromethane	0.28	0	349.0	342.7	560.0	213.6
diethyl ether	0.27	0	348.7	343.0	560.8	213.3
triethylamine	0.14	0	347.0	344.7	553.8	216.0
cyclohexane	0.00	0	347.2	344.5	551.8	216.8
n-hexane	−0.04	0	345.5	346.3	549.5	217.7
n-heptane	−0.08	0	346.5	345.2	551.4	216.9
Δ (DMSO-heptane)			12.2	−11.7	24.5	−9.2

[a] Values taken from ref 20. [b] log ϵ (dm^3 mol^{-1} cm^{-1}) = 4.21. [c] log ϵ (dm^3 mol^{-1} cm^{-1}) = 3.55. [d] Intransparent solvent.

nitronitrile. Compound **1** did not exhibit any discernible halochromism (lithium iodide in acetone) or preferential solvation in a toluene/2-propanol mixture. No measurable thermosolvatochromism was found, either (acetonitrile, ethyl acetate, *n*-hexane; 273 and 323 K).

For this analysis, the π^* and α parameters compiled by Marcus[20] were used which were derived by averaging data for several indicators. A revised π^* scale based on data for a single indicator was proposed.[21] However, two drawbacks of this revised scale are that no new π^* values are available so far for hydroxylic solvents and that α values were not redefined as well. Thus, a comparison of the old and new π^* scales was attempted using only non-HBD solvents. For E_{T1}, correlations with r^2 of 0.936 (old) and 0.946 (new), $N = 18$, and for E_{T2}, with r^2 of 0.954 (old) and 0.950 (new), $N = 20$, were obtained, respectively. Ultimately, a regression analysis was performed using the *SPP* and *SA* parameters of the Catalan scale[22] and yielded correlations with r^2 of 0.749 for E_{T1}, $N = 31$, and 0.781 for E_{T2}, $N = 32$ (no parameters were available for diiodomethane). In light of these results, the continuing use of the classic Kamlet−Taft parameters appears to be justified.

Moessbauer Spectroscopy. As is true of all neutral ferrocene-related organometallics having a single iron atom per formula unit, the spectra of **1** consist of well-resolved doublets. The line width (full-width half-maximum) for a thin absorber at 320 K is 0.234 ± 0.004 mm s^{-1}.

The isomer shift (IS) at 90 K is significantly smaller than that in ferrocene (0.509 compared with 0.531 mm s^{-1}). In the high-temperature regime (210−350 K), the temperature dependence is well fitted by a linear regression with r^2 of 0.998 for 9 data points. From the slope dIS/dT of $-(4.82 \pm 0.34) \times 10^{-4}$ mm s^{-1} K^{-1}, the calculated effective vibrating mass (M_{eff}) of the iron atom is 86 ± 8 daltons. The difference between this value and the "bare" iron value of 57 daltons is a reflection of the covalency of the metal atom-ligand bonding interaction and is very similar to those reported for other ferrocenoid solids.

The temperature dependence of the quadrupole splitting (QS) of the iron atom resonance is summarized graphically in Figure 2, and the value at 90 K is 2.249 ± 0.004 mm s^{-1}. This latter value is significantly smaller (by about 0.17 mm s^{-1}) than that reported for the parent compound ferrocene.[23] The QS goes through a maximum at ∼220 K which is suggestive of a structural change in the solid at approximately this temperature.

The temperature dependence of the recoil-free fraction, related to the mean-square amplitude of vibration of the metal atom, is summarized graphically in Figure 3. Again, in the high-temperature limit (210−350 K), the data are well represented by a linear regression with r^2 of 0.994 for 9 data points. From the slope d ln A/dT of $-(12.19 \pm 0.18) \times 10^{-3}$ K^{-1} and from the linear dependence of the IS parameter, the calculated Moessbauer lattice temperature (Θ_M) is 84 ± 4 K, justifying the high-temperature limiting calculations implied in these data. In this context, it is interesting to note that up to the 350 K maximum of the experiment (dictated by the very small resonance effect observable at high temperatures) there is no evidence of the type of vibrational amplitude anomaly (librational motion of the ring) which has previously been reported in octamethylferrocene and some derivatives.[24] Comparable ln $A(T)$ data for ferrocene have been reported in detail earlier.[25]

A final parameter which can be extracted from the Moessbauer data is the area ratio $R = [(A(+)/A(-)]$ of the two components of the doublet spectrum which is related to the

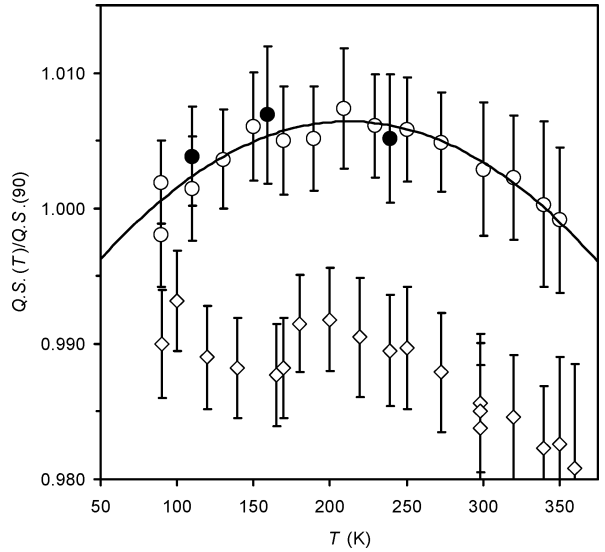

Figure 2. Temperature dependence of the quadrupole splitting parameter of **1** (○) and ferrocene (◊). The data have been normalized to the 90 K values for ready comparison, and the ferrocene data have been offset by −0.010 for clarity. The ferrocene data show the expected decrease in QS with increasing temperature (except for the discontinuity at the well-known λ-point at 163.9 K) due to thermal expansion. The three filled data points in the upper curve pertain to data acquired in a cooling mode (after acquiring the 350 K data) and reflect the reversibility of the data. The solid line represents the second-order polynomial regression through the data points.

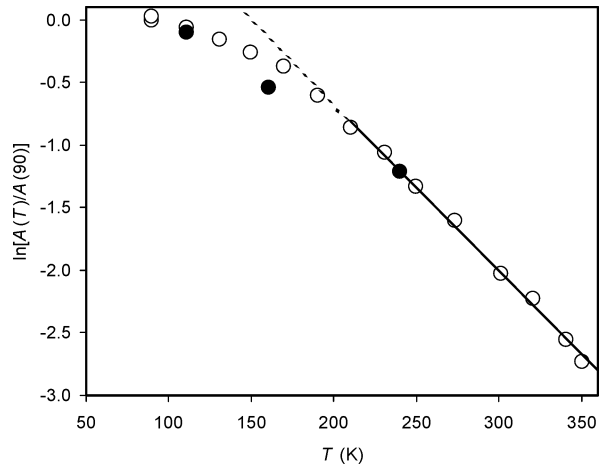

Figure 3. Temperature dependence of the area under the resonance curve for **1**. From the high-temperature slopes of the isomer shift and recoil-free fraction data, the calculated value of Θ_M is 84 ± 4 K. Symbols as in Figure 2.

anisotropy of the metal atom motion. The data show that the temperature dependence of this anisotropy is barely outside of experimental error. The nonunity value (∼0.96) in the low-temperature limit (90−150 K) probably reflects a small temperature-independent orientational effect (texture) in the sample, amounting to about 4−5% in the *R* values, as a consequence of the evaporation deposition from ether solution, as noted above.

As has been pointed out earlier,[26] from a knowledge of the temperature dependence of ln*A* extracted from the Mössbauer data, it is possible to calculate the root-mean-square-amplitude of vibration (rmsav) of the iron atom over the total temperature range of the measurements. Using the thermal factors ($U_{i,j}$) extracted from the X-ray data at 243 and 183 K as calibration points, this calculation has been effected for **1**, and the results are summarized graphically in Figure 4, in which the two X-ray

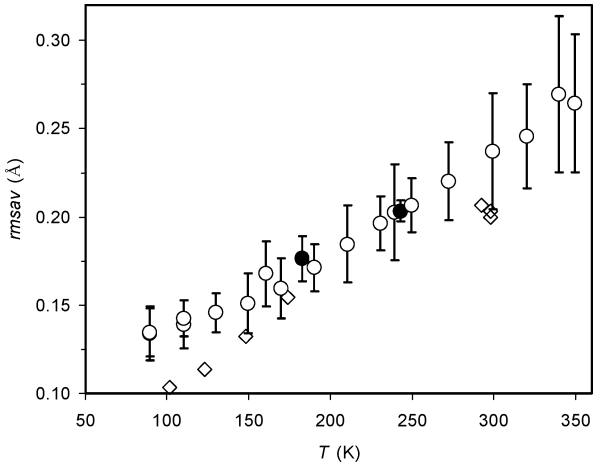

Figure 4. Root-mean-square-amplitude of vibration of the iron atom in **1** (○ from Moessbauer; ● from X-ray) and ferrocene (◊ from X-ray).

data points are indicated by the full circles. Also shown are the corresponding rmsav data for ferrocene, extracted from the X-ray data reported in the literature. The low-temperature data for ferrocene are complicated by the known crystallographic forms adopted by this parent material and should be considered with this in mind. The three high temperature points suggest that the *rmsav* of the metal atom in **1** is significantly larger than it is in ferrocene in the high-temperature regime.

These data can be understood on the basis of the following dynamics: below ∼150 K, the characteristics of the title compound are those of a "normal", primarily covalent, molecular solid. Above this temperature, ring rotation starts to become an observable dynamic and influences the mean-square-amplitude of the iron atom as reflected in the Moessbauer parameters. To be noted particularly is the maximum in the QS parameter at ∼220 K and the observations that both the temperature dependencies of the IS and ln *A* parameters are well fitted by linear regressions. The linearity of the latter suggests that the onset of ring rotation does not involve the type of "gear wheel" motion noted earlier in related octamethylferrocene complexes. Such motion would be evidenced in a marked nonlinearity of the ln *A* (*T*) dependence at the higher temperatures. Thus, this behavior is similar to that observed for the related 2-nitro-3-(octamethylferrocenyl)acrylonitrile.[9]

Differential Scanning Calorimetry. Moreover, the onset of ring rotation is reflected in the differential scanning calorimetry (DSC) data, which on heating show two overlapping endotherms at 228 and 236 K (peak maxima temperatures). The endothermic peaks are of similar size and shape (Figure 5), and the total enthalpy and entropy associated with these peaks are 0.26 kJ mol^{-1} and 1.13 J mol^{-1} K^{-1}, respectively. This enthalpy value is much smaller than those reported for the two polymorphic phase transitions of ferrocene,[27] which are 4.1 kJ mol^{-1} (transition at 242 K) and 0.9 kJ mol^{-1} (transition at 164 K). However, as discussed below, the overall crystal structure and molecular packing above and below the endothermic events at ∼ 230 K is basically the same but one kind of molecular disorder disappears below this temperature. It is obvious that this process is associated with less change in enthalpy than a more distinct change of the crystal structure which is true in the case of the ferrocene phase transitions. The splitting of the peak is likely due to a different transition kinetics of the concerned molecular units with slightly distinct environment in the low temperature form (four molecules in the asymmetric unit) which adopt a common kind of disordered arrangement in the room temperature form (two molecules in the asymmetric unit).

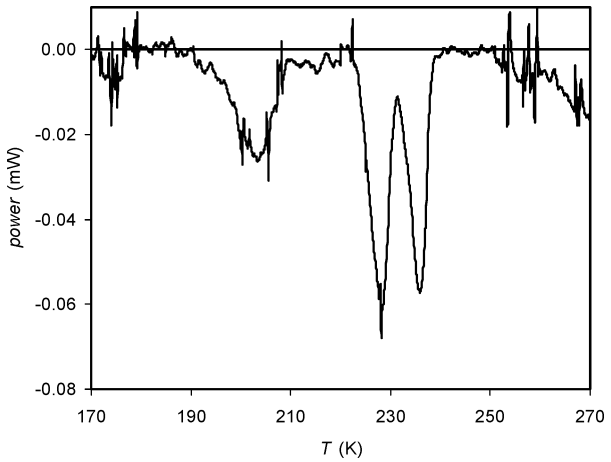

Figure 5. Baseline-corrected DSC plot of the title compound. The two endotherms are associated with the onset of ring rotation in the solid.

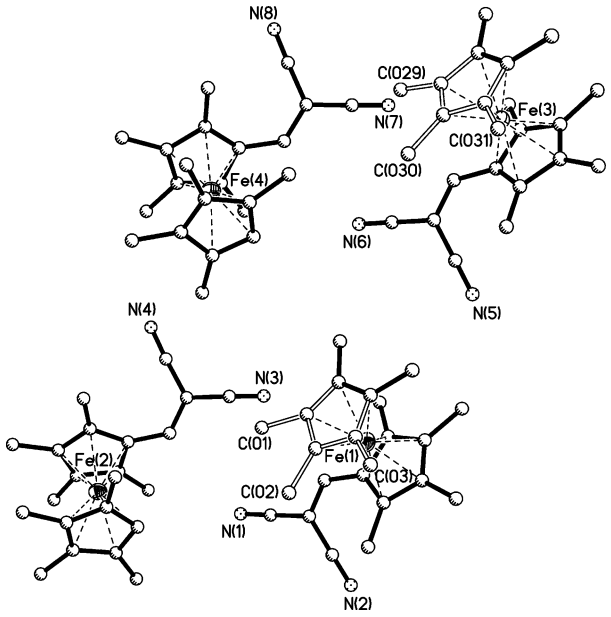

Figure 6. Crystal structure of **1** at 183 K.

X-ray Diffraction. The crystal structure shows that the conjugated π system deviates considerably from coplanarity by a dihedral angle of about 40°. This tilting may arise from crystal packing effects (in the related nitroacrylonitrile[9] the corresponding angle is only half this size).

As expected, differences in the X-ray diffraction data of a particular single crystal above and below the temperature of the phase transition support the Moessbauer results and provide impressive insight into the dynamic phenomena in the solid.

At 183 K, four molecules were found in the asymmetric unit with complete order of two molecules at Fe(2) and Fe(4) and an occupation disorder at the tetramethyl Cp rings for the others. Around Fe(1) and Fe(3), the Cp hydrogen atom is distributed in the ratio 60:20:20 over three positions, whereas around Fe(2) and Fe(4), the Cp rings adopt defined conformations. The torsion angles of the Cp rings at Fe(2) and Fe(4) are 15 and 30°, respectively (Figure 6).

The unit cell of the low temperature modification is nearly B-centered, except for orientation of the two Cp rings at Fe(2) and Fe(4). As a consequence, for the reciprocal lattice all reflections with $h + l = 2n + 1$ are systematically weak. By warming the crystal over 213 K, the Cp-rings at Fe(2) and Fe(4) reversibly twist from their defined conformations to two disordered positions, leading to an exact B-centered unit cell, which is not defined in a triclinic lattice system, with the extinction for reflections with $h + l = 2n + 1$. The 3×3 matrix to transform the low-temperature into the high-temperature triclinic unit cell is $-0.5, 0, -0.5; 0.5, 0, -0.5; -0.5, -1, -0.5$ (row by row) or the inverse matrix for the opposite direction with $-1, 1, 0; 1, 0, -1; -1, -1, 0$.

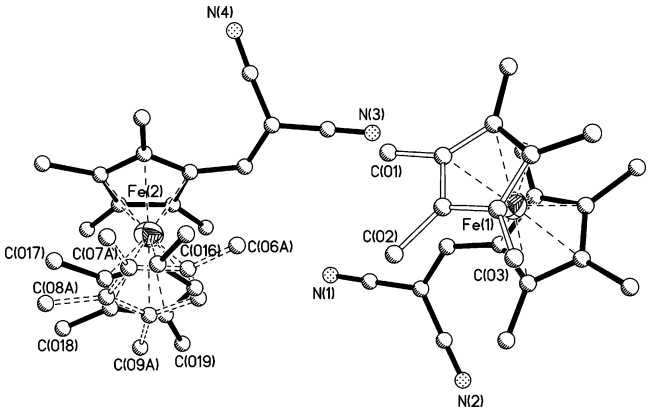

Figure 7. Crystal structure of **1** at 243 K.

At 243 K, two molecules were observed in the asymmetric unit with different kinds of disorder of the tetramethyl Cp rings. Around Fe(1), the Cp-hydrogen atom is distributed in the ratio 70:15:15 over three positions C(1), C(2), and C(3). Around Fe(2), there is a 1:1 disorder by twisting the ring by 36° (Figure 7).

Thus, by cooling the crystal below the temperature of the presumed onset of ring rotation, one kind of disorder can actually be frozen which formally doubles the number of molecules in the unit cell without changing their positions in the lattice. The remaining disorder cannot be interpreted as dynamic or statistical without ambiguity.

In contrast, a comparison of powder diffraction data at different temperatures did not reveal significant differences except for anisotropic shifts due to normal lattice contraction. Since, as rationalized above, the main difference between the two forms is the extinction of already weak reflections, unfortunately, X-ray powder diffraction is not a suitable analytical tool in this case to derive useful conclusions about the relevant phase transition phenomena.

Conclusions

Different complementary analytical techniques have contributed to an overall understanding of the structure, metal atom motion, conformational dynamics, and solvatochromism of a ferrocene-based short donor−acceptor conjugate both in solution and in solid state. Insight into the dynamic behavior was gained from the temperature dependence of Moessbauer and X-ray data. Due to the gap in the substitution pattern of one of the Cp rings, the conformational dynamics of (octamethylferrocenylmethylene)malononitrile are more intriguing than those of nonamethyl or pentamethyl analogues. With increasing knowledge about model compounds such as **1**, novel applications of these materials will be identified.

Acknowledgment. The authors are indebted to Ms. Janet Zoldan of the Technion-Israel Institute of Technology for her meticulous recording of the DSC data and to Prof. Karl-Hans Ongania of the University of Innsbruck for the mass spectra.

References and Notes

(1) Stankovic, E.; Toma, S.; Van Boxel, R.; Asselberghs, I.; Persoons, A. *J. Organomet. Chem*. **2001**, *637*−*639*, 426.

(2) Thomas, K. R. J.; Lin, J. T.; Wen, Y. S. *J. Organomet. Chem*. **1999**, *575*, 301.

(3) Calabrese, J. C.; Cheng, L.-T.; Green, J. C.; Marder, S. R.; Tam, W. *J. Am. Chem. Soc*. **1991**, *113*, 7227.

(4) Barlow, S.; Marder, S. R. *Chem. Commun*. **2000**, 1555.

(5) Herber, R. H. *Inorg. Chim. Acta* **1999**, *291*, 74.

(6) Alain, V.; Blanchard-Desce, M.; Chen, C.-T.; Marder, S. R.; Fort, A.; Barzoukas, M. *Synth. Met*. **1996**, *81*, 133. Alain, V.; Fort, A.; Barzoukas, M.; Chen, C.-T.; Blanchard-Desce, M.; Marder, S. R.; Perry, J. W. *Inorg. Chim. Acta* **1996**, *242*, 43. Janowska, I.; Zakrzewski, J.; Nakatani, K.; Delaire, J. A.; Palusiak, M.; Walak, M.; Scholl, H. *J. Organomet. Chem*. **2003**, *675*, 35.

(7) Reichardt, C. *Solvents and Solvent Effects in Organic Chemistry*, 3rd ed.; Wiley-VCH: Weinheim, Germany, 2002. Reichardt, C. *Chem. Rev*. **1994**, *94*, 2319.

(8) Laus, G.; Schottenberger, H.; Wurst, K.; Schütz, J.; Ongania, K.-H.; Horvath, U. E. I.; Schwärzler, A. *Org. Biomol. Chem*. **2003**, *1*, 1409.

(9) Laus, G.; Schottenberger, H.; Schuler, N.; Wurst, K.; Herber, R. H. *J. Chem. Soc., Perkin Trans. 2* **2002**, 1445.

(10) Herber, R. H.; Bildstein, B.; Denifl, P.; Schottenberger, H. *Inorg. Chem*. **1997**, *36*, 3586.

(11) Herber, R. H.; Nowik, I.; Schottenberger, H.; Wurst, K.; Schuler, N.; Müller, A. G. *J. Organomet. Chem*. **2003**, *682/1*−*2*, 163.

(12) Aresta, M.; Nobile, C. F.; Petruzelli, D. *Inorg. Chem*. **1977**, *16*, 1817.

(13) Özman, S. *Chem. Ztg*. **1976**, *100*, 143.

(14) Zou, C. H.; Wrighton, M. S. *J. Am. Chem. Soc.* **1990**, *112*, 7578.

(15) Barlow, S.; Bunting, H. E.; Ringham, C.; Green, J.; Bublitz, G. O.; Boxer, S. G.; Perry J. W.; Marder, S. R. *J. Am. Chem. Soc.* **1999**, *121*, 3715.

(16) Kamlet, M. J.; Abboud, J.-L. M.; Abraham, M. H.; Taft, R. W. *J. Org. Chem*. **1983**, *48*, 2877.

(17) Kamlet, M. J.; Hall, T. N.; Boykin, J.; Taft, R. W. *J. Org. Chem*. **1979**, *44*, 2599. Kamlet, M. J.; Abboud, J.-L. M.; Taft, R. W. *J. Am. Chem. Soc*. **1977**, *99*, 6027.

(18) Taft R. W.; Kamlet, M. J. *J. Am. Chem. Soc*. **1976**, *98*, 2886.

(19) Kamlet, M. J.; Taft, R. W. *J. Am. Chem. Soc*. **1976**, *98*, 377.

(20) Marcus, Y. *Chem. Soc. Rev*. **1993**, *22*, 409.

(21) Laurence, C.; Nicolet, P.; Dalati, M. T.; Abboud, J.-L. M.; Notario, R. *J. Phys. Chem*. **1994**, *98*, 5807.

(22) Catalán, J. In *Handbook of Solvents*; Wypych, G., Ed.; ChemTec: Toronto, 2001; p 583.

(23) Herber, R. H.; Nowik, I. *Hyperfine Interact.* **2001**, *136*, 699.

(24) Nowik, I.; Herber, R. H. *Inorg. Chim. Acta* **2000**, *310*, 191. Herber, R. H.; Nowik, I. *Hyperfine Interact.* **2000**, *126*, 127. Schottenberger, H.; Buchmeiser, M. R.; Herber, R. H. *J. Organomet. Chem*. **2000**, *612*, 1. Schottenberger, H.; Wurst, K.; Herber, R. H. *J. Organomet. Chem*. **2001**, *625*, 200. Herber, R. H.; Nowik, I. *Hyperfine Interact.* **2002**, *141/142*, 297.

(25) Gibb, T. C. *J. Chem. Soc., Dalton Trans.* **1976**, 1237. Herber, R. H.; Temple, K.; Manners, I.; Buretea, M.; Tilley, T. D. *Inorg. Chim. Acta* **1999**, *284*, 152.

(26) Herber, R. H.; Nowik, I. *Hyperfine Interact.* **2002**, *144/145*, 249.

(27) Dunitz, J. D. *Acta Cryst*. **1995**, B*51*, 619. Braga, D. *Chem. Rev.* **1992**, *92*, 633.